

Surface Characterization of Chromia for Chlorine/Fluorine Exchange Reactions

Ercan Ünveren,^{†,‡} Erhard Kemnitz,^{*,†} Andreas Lippitz,[‡] and Wolfgang E. S. Unger[‡]

Humboldt Universität zu Berlin, Institut für Chemie, Brook-Taylor Strasse 2, D-12489 Berlin, Germany, and Bundesanstalt für Materialforschung und -prüfung, Laboratorium VIII.23, D-12200 Berlin, Germany

Received: September 10, 2004; In Final Form: November 16, 2004

The dismutation of CCl_2F_2 was used to probe the effect of halogenation of chromia by Cl/F exchange reactions to find out the difference between the halogenated inactive and active catalysts. The heterogeneous reactions were performed in a continuous flow Ni reactor and also under simulated reaction conditions in a reactor where after the reaction X-ray photoelectron spectroscopy (XPS) and X-ray excited Auger electron spectroscopy (XAES) analyses are possible without air exposure of the catalyst, i.e., under so-called “in situ” conditions. The Cr(III) 2p XP spectra, which revealed multiplet splitting features and satellite emission, were used for chemical analysis by using a simple evaluation procedure which neglects this inherent complexity. Chemical analysis was also applied by using chemical state plots for Cr 3s in order to cross-check Cr 2p related results. Both ex and in situ XPS show that as soon as Cr_2O_3 is exposed to CCl_2F_2 at 390 °C fluorination as well as chlorination takes place at the catalyst surface. When the XPS surface composition reaches approximately 4 at. % fluorination and 6 at. % chlorination, maximum catalytic activity was obtained. Application of longer reaction times did not change significantly the obtained surface composition of the activated chromia. The fluorination and chlorination of chromia was further investigated by various HF and HCl treatments. The activated chromia samples and the Cr_2O_3 , $\text{Cr}(\text{OH})_3$, CrF_2OH , $\text{CrF}_3 \cdot \text{H}_2\text{O}$, $\alpha\text{-CrF}_3$, $\beta\text{-CrF}_3$, and CrCl_3 reference samples with well-known chemical structures were also characterized by X-ray absorption near edge structure (XANES), time-of-flight secondary ion mass spectroscopy (TOF-SIMS), pyridine-FTIR, wet chemical (F and Cl) analysis, X-ray powder diffraction (XRD), and surface area (BET) analysis. The results suggest that the formation of chromium oxide chloride fluoride species, e.g., chromium oxide halides, at the surface is sufficient to provide catalytic activity. The presence of any CrF_3 and/or CrCl_3 phases on the activated chromia samples was not found.

1. Introduction

The Cr_2O_3 is one of the most important catalysts in the chlorine/fluorine (Cl/F) exchange reactions; for example in the production of hydrofluorocarbons (HFC). Most of the reaction types in the synthesis of HFCs are basically halogen exchange reactions, e.g. fluorination (1), isomerization (2), and dismutation (3):



Chromia is established as an excellent heterogeneous catalyst for fluorination reactions.^{1–6} Although chromium(III) oxide is an important catalyst, the chemical nature and the active sites of the catalyst surface have not been completely investigated during these reactions. To study the chromia catalyst surface in detail, as a probe reaction for the catalytic halogen exchange, dismutation of CCl_2F_2 , was chosen because this has the advantage that the formation of HF in the course of catalytic reaction can be ruled out. It is well-known that activity of the oxide catalysts is achieved by exposure to fluorine containing

gases, e.g., fluoroalkanes, HF, SF_4 , etc.^{7–9} Drastic changes occur in the solid surface region due to the chemical reactions with the gas phase. Therefore, the main interest of this study was to find out which kind of modifications take place on the catalyst surface during conditioning and formation processes. Moreover, we were interested whether there are differences between the halogenated inactive and active catalysts and if there are separate phases or species formed like with Al_2O_3 catalyst samples activated by dismutation reactions of CCl_2F_2 ¹⁰ or if there are instead oxide-fluorides or mixed oxide-halides to be expected. This investigation was performed with samples which were activated in a continuous flow Ni reactor and also under simulated reaction conditions in a reactor with subsequent XPS analysis without air contact, providing so-called “in situ” conditions. Various analytical methods were applied and the results were compared with those of well-defined reference samples. Finally, it was the aim of this work to provide a better understanding on the basis of deeper insight in the conviction of the catalytically active fluorinated chromia phase or species as a result of activation of chromia by gaseous fluorine containing reactants.

2. Experimental Section

2.1. Sample Preparation. Reference Samples. Cr_2O_3 was synthesized by the volcano reaction of $(\text{NH}_4)_2\text{Cr}_2\text{O}_7$. To get rid of impurities the primary reaction product was boiled with distilled water for 4 h, filtered, washed with distilled water and

* Corresponding author. E-mail: erhard.kemnitz@chemie.hu-berlin.de. Fax: +49 30 2093 7277. Telephone: +49 30 2093 7555.

[†] Humboldt Universität zu Berlin.

[‡] Bundesanstalt für Materialforschung und -prüfung.

dried in air. Specific surface area (BET): 45.6 m²/g. XRD structure: PDF 38-1479.¹¹

Cr(OH)₃ was prepared by the addition of 0.1 M chromium nitrate to 0.25 M ammonia until a pH of 10.5 was reached. The gel obtained was allowed to settle. It was separated by centrifugation and then washed twice with distilled water and three times with acetone, slurried with diethyl ether, and again separated by centrifugation. It was dried for 24 h at room temperature in air.¹² Specific surface area (BET) was not detected, since Cr(OH)₃ decomposes above 100 °C. XRD structure: see ref 12.

CrF₃·H₂O was prepared from chromium(III) nitrate which was dissolved in slightly heated ethanol and then added dropwise to a stirred 40 wt % hydrofluoric acid solution. After 1 h the precipitate was separated, washed with water and ethanol and dried in air. Specific surface area (BET) was not detected, since CrF₃·H₂O decomposes above 100 °C. XRD structure: PDF 17-316.¹¹

CrF₂OH was synthesized by CrF₃·H₂O which was covered by aluminum foil to allow a self-produced atmosphere. Then, it was heated to 390 °C with a rate of 2 °C/min and kept at this temperature for 1 h under ~ 20 mL/min Ar flow. Specific surface area (BET): 1.5 m²/g. XRD structure: see refs 13 and 14.

β-CrF₃ was synthesized from (NH₄)₃CrF₆ which was covered by aluminum foil to allow a self-produced atmosphere. Then, it was heated to 490 °C with a rate of 3 °C/min and kept at this temperature for 2 h under ~ 20 mL/min Ar flow. Specific surface area (BET): 24.7 m²/g. XRD structure: PDF 80-555.¹¹

α-CrF₃ was obtained as a commercial product (Aldrich) received under Ar in a closed ampule. Specific surface area (BET): 0.4 m²/g. XRD structure: PDF 16-44.¹¹

CrCl₃ was obtained as a commercial product (Aldrich) received under Ar in a closed ampule. Specific surface area (BET): below the detection limit (<0.1) m²/g. XRD structure: PDF 32-279.¹¹

Catalyst Samples. Cr₂O₃ was dried in N₂ flow at 400 °C for 3 h, before activation or halogen treatment.

(i) Dried chromia was activated by a dismutation reaction of CCl₂F₂ at 390 °C for 1, 2, 3, 4, 5, 10, 15, 30, 120, 180, 540, 900, and 1440 min in a tubular flow reactor.

(ii) Dried chromia was activated by a dismutation reaction of CCl₂F₂ at 300 °C for 15, 25, 30, 45, and 120 min in a tubular flow reactor.

(iii) Dried chromia was activated by dismutation reaction of CCl₂F₂ at 390 °C for 1, 3, 5, and 9 h under “in situ” conditions.

(iv) Dried chromia was treated by HF or HCl at 390 °C for 15, 60, 180, and 540 min in a tubular flow reactor.

(v) Dried chromia was treated first by HF then by HCl and vice versa at 390 °C for 15 + 15 min in a tubular flow reactor.

(vi) Dried chromia was treated first by HF or HCl and then activated by CCl₂F₂ at 390 °C for 15 + 60 min in a tubular flow reactor.

2.2. Activation and Halogen Treatment. Dismutation of CCl₂F₂ Under Steady Flow Conditions. Cr₂O₃ catalyst samples were prepared with corn sizes of 0.3–0.5 mm by pressing under 5t and sieving. Approximately 0.4 g catalyst was set into a vertical nickel reactor of length 400 mm and inner diameter 5 mm. The catalyst was held in the middle of the reactor by a piece of silver wool. The reactor (cf. Figure 1, right) was heated in a cylindrical resistance oven which was equipped with a temperature controller. The flow of CCl₂F₂ and N₂ was adjusted with mass flow controllers (MKS instruments) to 2 and 10 mL/min, respectively so that the residence time was about 2 s. The

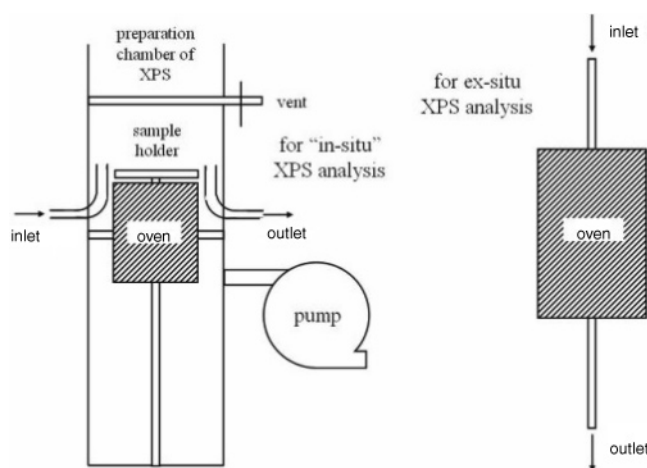


Figure 1. Scheme of reactor mounted to the preplock of ESCALAB 200X spectrometer for “in situ” XPS analysis (left) and tubular flow reactor for ex situ XPS analysis (right).

lining to and from the reactor was made with PTFE tubes which were also heated with heating bands in order to prevent any condensation. The outlet was directly connected to a GC where the amount of dosing was controlled by a specific valve. After each reaction the catalyst samples were taken from the reactor into the glovebox avoiding air exposure. They were transferred in an evacuated desiccator to the spectrometer. After the samples were placed into the spectrometer with only a few seconds of air exposure, the chamber was pumped down to UHV and the analyses were performed under these vacuum conditions.

Dismutation of CCl₂F₂ Under “in situ” Conditions. The reactions were also performed in a reactor which was directly mounted to the extended preplock chamber of the XP spectrometer. The reactor (cf. Figure 1, left) was separated by a valve from the extended preplock chamber and that was separated from the measuring chamber by another valve. The effluent gas was collected in glass containers for online GC analysis.

After each reaction the reactor was pumped down to UHV so that the activated catalyst sample was transferred first to the extended preplock chamber and then to the spectrometer without any air contact. This mode of analysis is often but not correctly called “in situ” analysis.

HF and HCl Treatment. HF and HCl treatment of chromia was applied in the tubular flow reactor at similar conditions and the samples were handled after the treatment as described above.

2.3. Analytical Methods. X-ray Photoelectron Spectroscopy (XPS). XP spectra were acquired with a VG SCIENTIFIC ESCALAB 200X electron spectrometer. X-ray photoelectron and X-ray excited Auger electron wide and narrow scan spectra were acquired using nonmonochromatized Al K α excitation operated at 15 kV and 20 mA. Wide and narrow scans were recorded in CRR 10 and CAE 10 modes, respectively. Cr LMM narrow scan XAES was acquired in CAE 20 mode. The vacuum in the spectrometer was in the range of 10⁻⁹ mbar during the measurements. The spot size was adjusted to a diameter of 3 mm. Binding or kinetic energy data were referenced to the aliphatic C 1s peak at 284.8 eV.¹⁵ No flood gun was used for charge compensation. The spectrometer energy scale was calibrated following ISO 15472.¹⁶ For the spectral analysis and chemical interpretation the softwares Unifit 2003 (University Leipzig, Leipzig, Germany) and Eclipse 2.0 (VG Scientific, U.K.) were used.

X-ray Absorption Near Edge Structure (XANES). XANES spectra at the Cr K-edge of the reference and activated samples were acquired in the transmission mode at a hard X-ray beamline, BAMline, at BESSY II. In the experiments a double multilayer monochromator, which consists of a stack of 150 W/Si layers ($d = 2.8$ nm) covering the photon energy range 4 to 40 keV, was used. A monoenergetic photon flux with maximum density of 1012 photons/s \cdot mm² and an energy resolution of 10 eV was obtained. For the analysis of the XANES spectra the WINXAS (Version 3.0) software was used. The background correction and the normalization of the Cr K-edge XANES spectra were done by using two polynomial fits each of order 1.

FTIR—Photoacoustic Analysis. The photoacoustic spectrum was recorded by FTIR-System 2000 from Perkin-Elmer where the METC 300 photoacoustic unit was mounted. Approximately 80 mg sample was charged in it and treated with two times 30 μ L of pyridine at 150 °C for 15 min in a vertical flow reactor where 10 mL/min Ar as carrier gas was used. After the treated sample was cooled to room temperature, it was transferred into the photoacoustic unit. The sample was flushed with He for 10 min. All spectra were normalized to 100% transmission.

Wet Chemical Analysis. Fluorine Analysis. Since the samples were not soluble, they were decomposed in concentric acids. Therefore, amounts of 20–60 mg of samples were melted with a mixture of 500 mg of Na₂CO₃ and 500 mg of K₂CO₃ in a Pt-pot for 20 min. After cooling, the obtained mixtures were dissolved in concentric H₃PO₄ or H₂SO₄. The determination of F concentration was carried out according to Seel¹⁷ using a fluoride sensitive electrode.

Chlorine Analysis. A solution of 4 mL of H₂O and 5 drops of H₂O₂ was prepared in a volumetric flask. The sample was added to this solution and after 30 min it was washed with 20 mL of alcohol and 0.5 mL of nitric acid (0.5 N). Two drops of 1 wt % diphenylcarbazone (DPC) was added and the titration was followed with mercury(II) chloride (0.01 N). Thus, the DPC acts as an indicator, changing from pink to blue when the first excess of mercury(II) appears.

Powder X-ray Diffraction (XRD). XRD of the powder samples were performed with Cu K α excitation using the XRD 7, Bragg–Brentano geometry with Ni filter, from Seiffert-FPM.

Surface Area Analysis (BET). Surface area of the samples were analyzed with N₂ (99.999%) according to the BET method using ASAP 2000 from Micromeritics. The samples were degassed at 250 °C until high vacuum conditions were reached (~ 10 –5 mbar).

Gas Chromatography (GC). The organic reaction products were determined by GC Shimadzu 14a using 10% SE 30 Chromosorb column and flame ionization detector (FID). The retention times for the organic products, CClF₃, CCl₂F₂, CCl₃F, and CCl₄ were determined as 4.5, 5.0, 7.2, and 11.6 min, respectively.

3. Results and Discussions

3.1. Activation Studies. The dismutation of CCl₂F₂, which is a consecutive reaction and is given by eqs 4 and 5, was used to probe the effect of Cl/F exchange reactions on activation of chromia in order to find out how the inactive catalyst changes to an active catalyst.

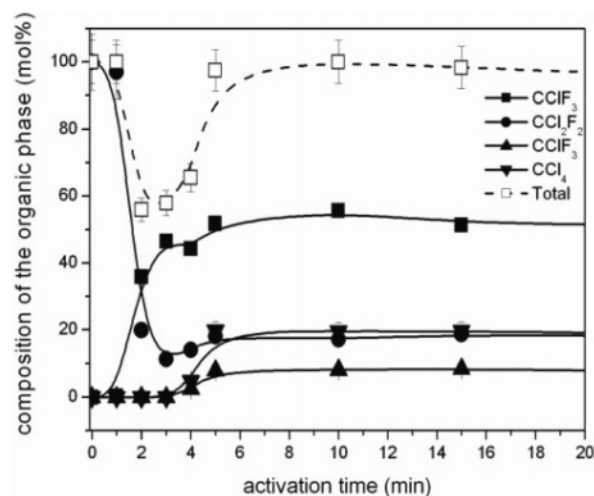


Figure 2. Cr₂O₃ catalyzed dismutation reaction of CCl₂F₂ at 390 °C.

As it is well established in the literature¹⁸ chromia requires an activation (formation) process before it becomes catalytically active. The time dependent change of concentrations of the reactant and the dismutation products was followed by gas chromatography (GC). As it can be seen from Figure 2, at 390 °C the catalyst starts at about 1 min after introducing the CCl₂F₂ to become active and within 5 min it reaches full catalytic activity. About 80% of CCl₂F₂ is converted to products. At 300 °C, a similar behavior was observed. However, due to the lower temperature, it takes nearly 20 min until the catalyst is getting active. Also a shift in the dismutation equilibrium was observed (conversion ca. 60%) which is mainly due to the temperature resulting in a lower catalytic activity of the reaction system.

The overall Cl/F mole ratio of the halocarbons should be one when only the dismutation reaction takes place. Since it deviates from one until the full catalytic activity was reached, another phenomenon, which is the formation process, accompanies the dismutation reaction. Higher fluorinated dismutation products and HCl were released as higher chlorinated dismutation products were decomposed, therefore not in the effluent observed until the full catalytic activity was reached.

To prevent the air contamination, the dismutation reaction of CCl₂F₂ at 390 °C was also performed under simulated reaction conditions. After the reaction, the activated chromia samples were transferred into the XP spectrometer without exposure to air. Here, the time until catalytic activity was achieved was longer when compared with the one in the tubular flow reactor due to the large reactor volume. The catalytic activity was also followed in this experiment by the product ratios which were determined by the GC analysis.

3.2. FTIR—Photoacoustic Analysis. The use of pyridine to determine the nature of acidity on solid surfaces has been well established.^{8,19} The lone-pair electron of the nitrogen atom of pyridine can either bind coordinatively to Lewis acid sites (LPy) or interact with acidic OH groups to form pyridinium cations or pyridine adsorbed via hydrogen bridge bonds, Brønsted sites (BPy). The 19b and 8a ring vibration modes of the pyridine molecules are very sensitive for distinguishing between adsorption on Lewis acid sites and that on Brønsted acid sites:

(1) Between the wavenumbers 1445 and 1455 cm⁻¹, the 19b ring vibration mode of pyridine, which is coordinatively bonded to Lewis acid sites (LPy), is observed.

(2) At about 1493 cm⁻¹, 19a ring vibration mode of pyridine is observed. This pyridine is either coordinatively bonded to Lewis acid sites (LPy) or bonded to Brønsted acid sites (BPy).

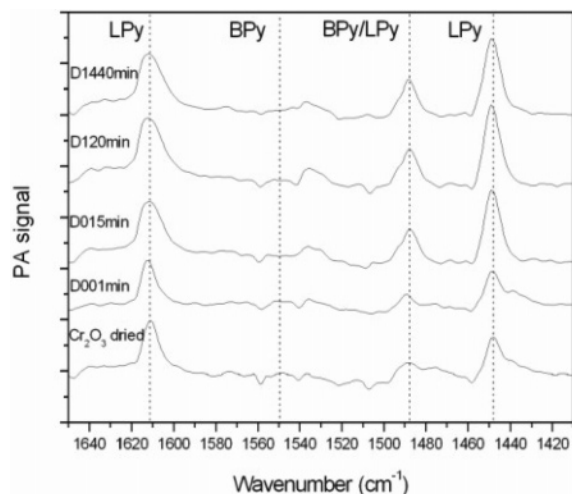


Figure 3. FTIR photoacoustic spectra of pyridine chemisorbed Cr_2O_3 samples activated at 390 °C.

(3) Between the wavenumbers 1540 and 1550 cm^{-1} , the 19b ring vibration mode of pyridine corresponds to hydrogen bonded pyridine to quasi-Brønsted acid sites (BPy).

(4) At about 1615 cm^{-1} , the 8a ring vibration mode of pyridine, which is coordinatively bonded to Lewis acid sites (LPy) of lower strength, is observed.

(5) At about 1620 cm^{-1} , the 8a ring vibration mode of pyridine, which is coordinatively bonded to Lewis acid sites (LPy) of higher strength, is observed.

Figure 3 presents characteristic FTIR-spectra of activated samples. The band at approximately 1490 cm^{-1} appears due to Lewis acid sites only. Since Brønsted acid sites are not found between the wavenumbers 1540 and 1550 cm^{-1} , the band at about 1493 cm^{-1} appears due to Lewis acid sites. There are no Brønsted acid sites present. Comparison the activated samples with the dried one reveals very slight increase in the number of the Lewis acid sites as well as very small shifts to the higher wavenumbers.

3.3. Wet Chemical Analysis. In previous studies Kemnitz et al.²⁰ showed that the chemical analysis reveals 0.5 wt % fluoride and 0.4 wt % chloride in the conditioned chromia. In another investigation Hess et al.⁸ reported slight chlorination (1–2 wt % chloride) and very small fluorination (about 0.3 wt % fluoride) in the activated samples. These results are consistent with the ones tabulated in Table 1. Wet chemical analysis and XPS show the same trend in halogenation of the samples, but comparison of these results indicates clearly that the halogenation takes place merely on the surface.

3.4. XANES. The X-ray pattern of the activated samples are in agreement with the X-ray pattern of the reference Cr_2O_3 (PDF 38-1479, Eskolite) but the reflection intensities are slightly reduced and the signal-to-noise ratios are decreased. The crystalline bulk properties are not significantly changing with activation. That means, either the new phases are X-ray amorphous or the changes are concentrated at the very surface.

To check this, XANES measurements of the activated samples were undertaken at the Cr K-edge in transmission mode. The XANES spectra of the reference samples presented in Figure 4 differ from each other in their preedge and near-edge features. As the peaks in the preedge region represent the resonant dipole-forbidden Cr 1s \rightarrow 3d transition, the first peak which appears after the edge jump in the near-edge region represents the dipole-allowed Cr 1s \rightarrow 4p transition. The peaks following this one in the near-edge region appear due to multiple scattering processes.²¹ The detailed description of the features in the XANES

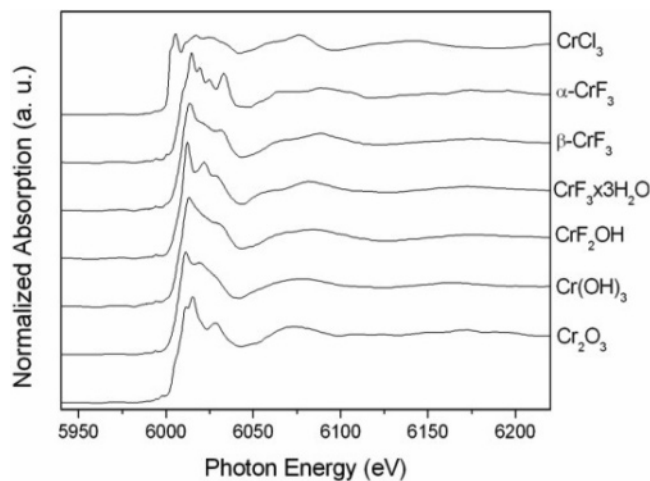


Figure 4. Cr K-edge XANES in transmission mode for reference samples.

TABLE 1: Comparison of Wet Chemical Analysis (Top) with ESCA (Bottom)

reaction	temp (°C)	time (min)	F (wt %)	Cl (wt %)	overall composition
dismutation	300	15	0.1	1.3	$\text{CrO}_{1.48}\text{F}_{0.00}\text{Cl}_{0.03}$
dismutation	300	120	0.6	2.0	$\text{CrO}_{1.47}\text{F}_{0.02}\text{Cl}_{0.04}$
dismutation	390	1	0.2	0.9	$\text{CrO}_{1.49}\text{F}_{0.01}\text{Cl}_{0.02}$
dismutation	390	15	0.5	1.8	$\text{CrO}_{1.47}\text{F}_{0.02}\text{Cl}_{0.04}$
dismutation	390	120	0.7	1.9	$\text{CrO}_{1.47}\text{F}_{0.03}\text{Cl}_{0.04}$
dismutation	390	1440	0.7	2.4	$\text{CrO}_{1.46}\text{F}_{0.03}\text{Cl}_{0.05}$
HF treatment	390	15	1.5	0.0	$\text{CrO}_{1.47}\text{F}_{0.06}$
HCl treatment	390	15	0.0	1.8	$\text{CrO}_{1.48}\text{Cl}_{0.04}$

reaction	temp (°C)	time (min)	F (at. %)	Cl (at. %)	XPS surface composition
dismutation	300	15	0.7	1.3	$\text{CrO}_{1.42}\text{F}_{0.02}\text{Cl}_{0.03}$
dismutation	300	120	4.9	5.6	$\text{CrO}_{1.39}\text{F}_{0.13}\text{Cl}_{0.15}$
dismutation	390	1	1.6	2.2	$\text{CrO}_{1.59}\text{F}_{0.04}\text{Cl}_{0.06}$
dismutation	390	15	4.1	6.7	$\text{CrO}_{1.48}\text{F}_{0.11}\text{Cl}_{0.18}$
dismutation	390	120	5.1	6.8	$\text{CrO}_{1.26}\text{F}_{0.13}\text{Cl}_{0.17}$
dismutation	390	1440	5.1	6.2	$\text{CrO}_{1.31}\text{F}_{0.13}\text{Cl}_{0.16}$
HF treatment	390	15	11.5	0.0	$\text{CrO}_{1.13}\text{F}_{0.28}$
HCl treatment	390	15	0.0	6.1	$\text{CrO}_{1.24}\text{Cl}_{0.14}$

spectra and the relation to the chemical structure of some of the references are explained by Böse et al.²² in a previous paper. When the XANES spectra of the treated and activated samples are compared with the spectra of the references, it is seen that they look very similar to the spectra of Cr_2O_3 and very different from the spectra of other references (cf. Figures 5 and 6). This ensures that all the activated and treated samples are in Cr_2O_3 structure, because the transmission mode experiments provide information from bulk and surface, mainly from the bulk. Therefore, the chemical alterations due to the formation of new species with treatment or activation should be restricted to the very surface of the samples. The chemical composition of the HF treated sample, which possesses the highest fluorine content undertaken in XANES analysis, is $\text{CrO}_{1.47}\text{F}_{0.06}$. Also, Adamczyk et al.²³ could not observe any clear differences in the XANES spectra for such low fluorine containing oxide fluoride samples which were prepared by thermal decomposition of a mixture of $(\text{NH}_4)_3\text{CrF}_6/\text{Cr}_2\text{O}_3$.

3.5. XPS. Since all the determined BET surface areas were significantly low, XPS provides surface information. Table 2 shows the XPS surface compositions of the activated catalyst samples at 390 °C. Relying on these data the catalytic activity starts significantly when the chromia surface is by 1.6 at. % fluorinated and by 2.2 at. % chlorinated. When the F and Cl

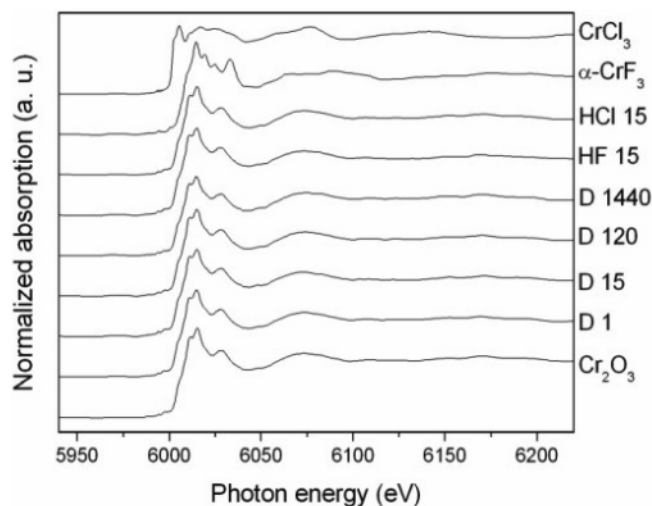


Figure 5. Cr K-edge XANES spectra of activated Cr_2O_3 samples compared to the spectra of Cr_2O_3 , CrF_3 and CrCl_3 .

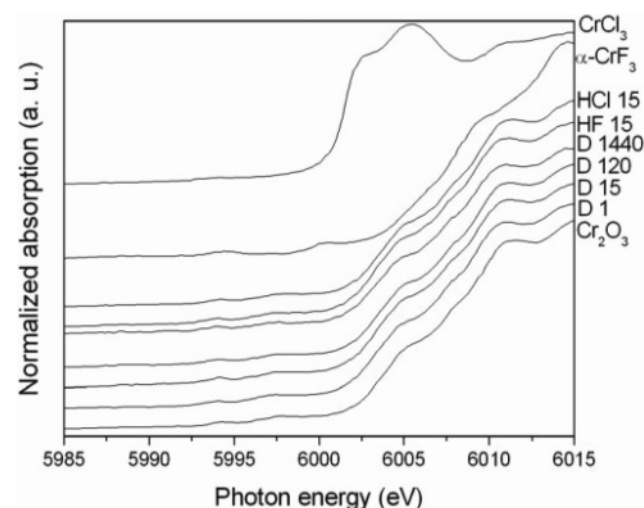


Figure 6. Pre-edge structure of Cr K-edge XANES spectra of activated Cr_2O_3 samples compared to the spectra of Cr_2O_3 , CrF_3 , and CrCl_3 .

TABLE 2: XPS Surface Composition (at. %) of Cr_2O_3 Catalysts Activated with CCl_2F_2 Dismutation Reaction at 390 °C

time (min)	F	Cr	O	Cl	F + Cl	activity of catalyst
0	0	42.9	57.1	0	0	inactive
1	1.6	37.1	59.1	2.2	3.7	inactive
2	1.7	38.3	55.1	4.8	6.6	partially active
3	3.7	38.3	52.4	5.6	9.3	partially active
4	3.6	39.5	50.8	6.1	9.7	partially active
5	3.7	39.9	50.7	5.7	9.4	partially active
10	4.1	38.6	51.0	6.3	10.5	fully active
15	4.1	36.1	53.2	6.7	10.7	fully active
30	4.7	38.8	51.8	4.6	9.4	fully active
120	5.1	39.0	49.0	6.8	11.9	fully active
180	5.3	38.6	49.5	6.7	12.0	fully active
540	5.6	38.8	49.7	5.9	11.5	fully active
900	5.3	38.6	49.6	6.6	11.9	fully active
1440	5.1	38.4	50.3	6.2	11.3	fully active

contents at the catalyst surface have reached ca. 4 and 6 at. %, respectively, the highest activity is established. However, once the maximum activity was achieved there was no drastic further damage of surface composition of the catalysts with increasing reaction time. Even after 24 h of reaction time, only 5.1 at. % fluoride and 6.2 at. % chloride was found on the solid surface. The predried chromia which still possesses OH groups on the surface reacts with dismutation products. Since the higher

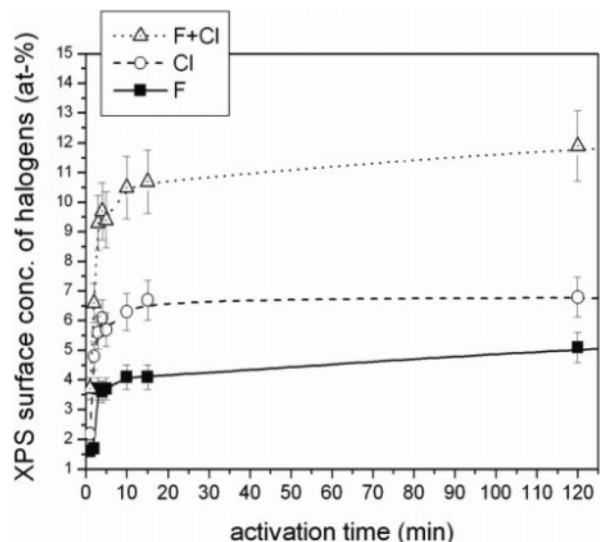
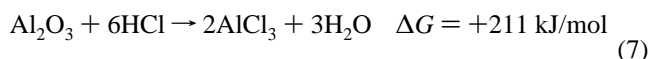


Figure 7. Change in XPS halogen concentration on chromia surface with reaction time.

chlorinated dismutation products are more reactive than the higher fluorinated ones, they decompose and HCl was released with the other formation products.²⁴ Therefore, a higher degree of chlorination than fluorination was found on the surface. The rapid halogenation of the surface took place until the OH groups and adsorbed water was removed from the chromia surface. After that point, further halogenation of the solid surface slowed. Although the fluoride concentration did not exceed the chloride concentration by further halogenation of the surface, a relative increase was observed in the long run (cf. Figure 7). These results are different than the ones obtained with activated alumina. Böse et al.¹⁰ reported that 10 at. % fluorination was reached until the full catalytic activity was established. In the case of alumina, fluorination continues until full conversion into the fluoride has taken place. There is no significant chlorine uptake because the chlorination of alumina is not favored thermodynamically (cf. eq 7). In contrast to the alumina system, in the case of chromia this process is coming to an end at total halogen concentration of about 10%.

These differences between alumina and chromia can be understood based on the thermodynamically different situations in both systems. The Gibbs free energies of the hydrofluorination and hydrochlorination reactions of chromia are almost similar,¹⁸ and therefore they are competitive with each other. Contrary, in the case of alumina fluorination is strongly dominating over the chlorination.



In XPS the common practice is to apply an appropriate fit procedure to analyze the spectrum in order to find out the BE of the photoelectrons of the relevant species states. Since static charging takes place for insulating materials, a reliable static charge referencing is required. The C 1s BE for aliphatic carbon (284.8 eV), which is present in solid materials due to contamination, is usually referenced to in the literature.¹⁵

The activated chromia samples were halogenated and therefore, different chemical states might be expected in the spectra.

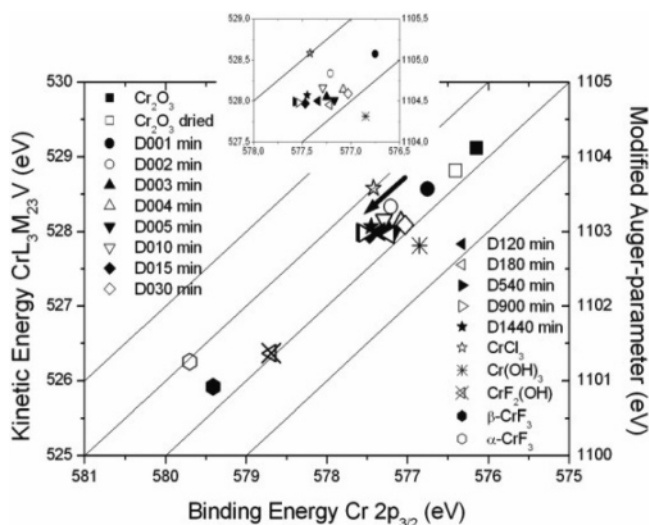


Figure 8. Chemical state plot for Cr $2p_{3/2}$ of Cr_2O_3 samples activated at 390°C .

However, as described in ref 25 because of the complicated spectral features of Cr 2p it is cumbersome to follow such a fitting procedure for all possible chemical states meaning that to handle with many peaks at the same time. This was not applicable, and if it were, no unequivocal results would be obtained. Since the chromia was the major compound and the fluorine and chlorine atomic concentrations were not so high, taking the BE of the corresponding maximum point in Cr $2p_{3/2}$ spectrum directly or by applying the fit procedure according to ISO 15472¹⁶ might be a good solution. Directly taking the KE at the maximum point of a complicated Auger transition is a known practice in XPS. On the other hand, Cr 3s can be alternatively a good candidate for XPS, although it has relatively low intensity. It has a much simpler spectrum than Cr 2p. Therefore, the chemical states were also determined alternatively from Cr 3s spectrum by applying an appropriate fit procedure in order to verify the validity of the results which were obtained from Cr 2p BEs. Cr 2p BE data are common standards in XPS analysis for chromium because of the intense signal. The results of the relevant photoemission data obtained for the catalyst samples activated at 390°C with a dismutation reaction of CCl_2F_2 and for the reference samples were presented in a chemical state plot (cf. Figure 8) according to Wagner and Joshi.²⁶

For Cr 2p, different chemical states were distinguished. In particular, the dried chromia has a higher BE than the untreated one. Thermal dehydroxylation of the fresh chromia increases the BE from 576.15 to 576.40 eV. Because of the drying process the hydroxyl groups and adsorbed water which saturate the metal sites were removed resulting in coordinatively unsaturated Cr(III) at the surface. This positive partial charge at the chromium atoms were the reason for that shift in BE. It attracts valence electrons of the neighbor oxygen atoms causing an increase in the BE in core levels of the oxygen as well. A shift of 0.40 eV was observed for the O 1s BE. The O 1s spectrum of fresh chromia had an asymmetry at the high binding energy side. It consisted of two subpeaks with binding energies at 529.85 and 532.00 eV which are characteristic for O of metal oxide and OH groups, respectively.²⁷ The relative peak areas of the hydroxide are reduced from 9.1% to 2.9% of the total O 1s signal by thermal dehydroxylation.

For the catalyst sample obtained by the dismutation reaction at 390°C for 1 min, a further increase in the Cr $2p_{3/2}$ BE by 0.35 eV was observed at constant α' . After 2 min activation

time, the Cr $2p_{3/2}$ line shifts further to higher BE by 0.45 eV, and until the maximum activity was reached, there was no further significant change in the Cr $2p_{3/2}$ BE. Further slight increases were observed in the Cr $2p_{3/2}$ BE with increasing reaction time. Maximal 0.3 eV shifts were found in the Cr $2p_{3/2}$ BE up to 24 h reaction times. Since the Cr–F and Cr–Cl bonds are stronger than Cr–O and Cr–OH bonds, an increase of the Cr $2p_{3/2}$ BE is to be expected.

Once the formation process was completed further fluorination and chlorination of the first layers of the crystal lattice proceeds slowly. The oxygen/halogen exchange increases also the Cr $2p_{3/2}$ BE, especially due to the replacement of less electronegative oxygen by a more electronegative fluorine. Inspection of the shape of the Cr 2p spectra did not reveal any significant alteration. There was no indication of either broadening of the spectrum, growth of a shoulder or of another emission line. This indicates that within the detection limits of XPS no nucleation of a separate fluorine and chlorine containing phase in the Cr_2O_3 matrix takes place. In addition, α' for Cr $2p_{3/2}$ does not change significantly meaning that the extra atomic relaxation energy is not changing and therefore the chemical shifts can be considered in terms of initial state effects. The halogenation of the Cr_2O_3 increases the positive charge at the chromium metal site because fluorine is more electronegative than oxygen. All these catalyst samples lay between the data points of chromia and chromium fluorides in the chemical state plot of Cr $2p_{3/2}$. They are more on the Cr_2O_3 position and far away from α - and β - CrF_3 . The conclusion is that, oxide–fluoride or oxide–halide species were formed on the catalyst surface.

The same conclusion can also be derived when the satellite of Cr $2p_{1/2}$ in the Cr 2p XP spectrum is considered. The BEs of these satellites were found to be 596.7, 597.0, and 601.0 eV for CrCl_3 , Cr_2O_3 and α - CrF_3 , respectively (see ref 28). For the activated Cr_2O_3 samples the BE values of Cr $2p_{1/2}$ satellites in the Cr 2p spectra are around 598.00 ± 0.25 eV, which are absolutely different from the Cr $2p_{1/2}$ satellite BEs of the references. Hence, formation of chromium oxide halide species are expected at the surface.

As mentioned above, a similar chemical state plot of Cr 3s for the activated and reference samples are also presented in Figures 9. The Cr 3s spectra of the chromium(III) compounds of O, F, and Cl show also multiplet splitting due to the interactions between the positively ionized core hole and singly filled d orbitals. However, compared with the Cr 2p spectra they are much simpler and can be fitted using a doublet with an intensity ratio of 2:1 and an energy separation of 4.0 eV. The reference samples were fitted with these constraints and the BE of the higher intensity multiplet was taken for the chemical state plot. In the literature,²⁹ it is reported that the Cr 3s levels for the insulators also display weak satellite features. In our study these features were so weak that these were not observable and therefore not considered in the spectral chemical analysis. For the activated samples one doublet was set with the initial parameters obtained for the Cr 3s level of Cr_2O_3 with intensity ratio of 2:1. Consequently, the Cr 3s binding energies for the Cr–O bond were plotted into the Wagner plots. Figure 9 shows clearly that the Cr 3s BE in this bond increases continuously with thermal dehydroxylation and further halogenation.

This causes a higher positive charge at the metal sites, and therefore an increased Lewis acidity (also cf. Figure 3). These results support the ones extracted from the Cr $2p_{3/2}$ chemical state plots as well.

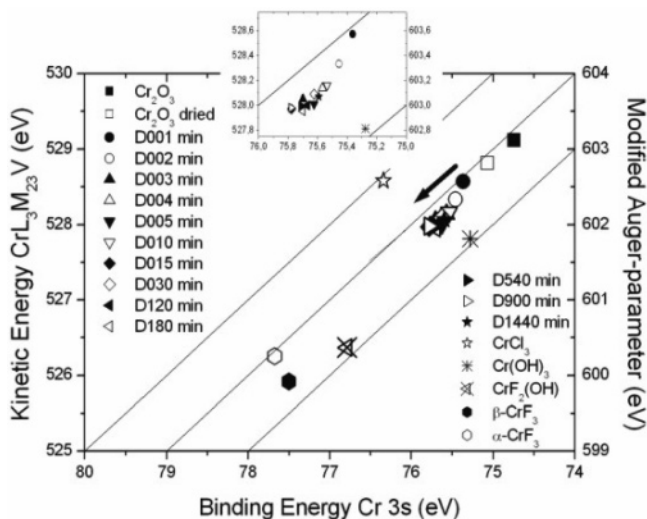


Figure 9. Chemical state plot for Cr 3s of Cr_2O_3 samples activated at $390\text{ }^\circ\text{C}$.

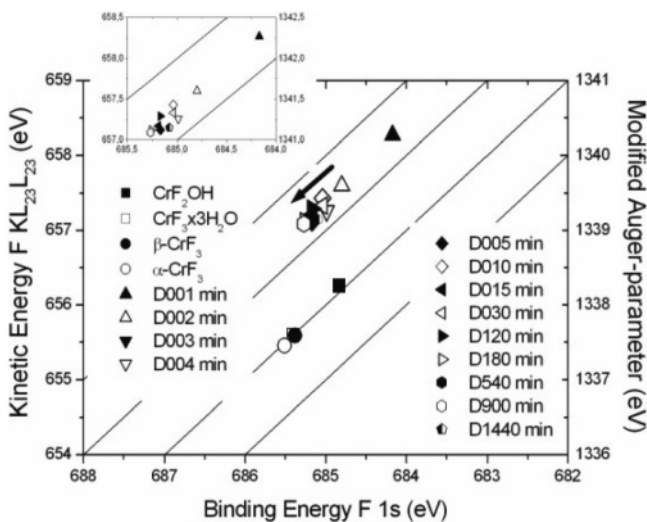


Figure 10. Chemical state plot for F 1s of Cr_2O_3 samples activated at $390\text{ }^\circ\text{C}$.

The F 1s BE is 684.15 eV for the inactive catalyst (cf. Figure 10). This indicates a comparatively high negative charge at the F ions in this stage. This means, these fluorine atoms are strongly basic in nature. As soon as the catalytic activity starts (within 2 min), the F 1s BE increases to 684.80 eV, and with further reaction time, the F 1s BE increases gradually. When the catalyst is activated by CCl_2F_2 at $390\text{ }^\circ\text{C}$ up to 24 h, F 1s BE reaches to a maximum value of 685.25 eV. Within the first 2 min, the catalyst surface undergoes a dramatical change so that the F 1s BE increases by 0.65 eV relative to the F 1s BE of the inactive sample. The electron density of F relatively decreases as it further integrates to the subsurface region. The atomic environment of the integrated F ions are different than the ones at the uppermost surface. The electron density will be reduced and so the core level F 1s BE increases. After this stage the fluorination of the chromia takes place slowly, therefore, the F 1s BE increases only slightly. The modified Auger parameters of F 1s are unchanged for the activated samples, therefore, the increase in F 1s BE can be discussed in terms of initial state effects. It is clearly seen that the activated catalysts are very different from the $\alpha\text{-CrF}_3$, $\beta\text{-CrF}_3$, CrF_2OH , and $\text{CrF}_3\cdot\text{H}_2\text{O}$ reference samples. The catalytically active species are different than these phases.

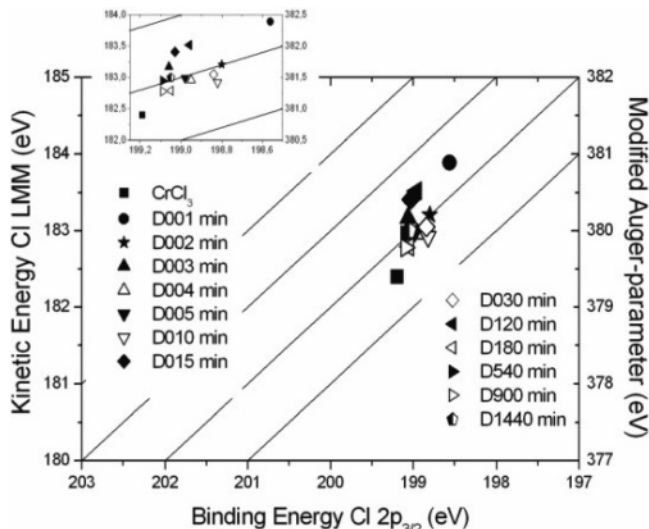


Figure 11. Chemical state plot for Cl $2p_{3/2}$ of Cr_2O_3 samples activated at $390\text{ }^\circ\text{C}$.

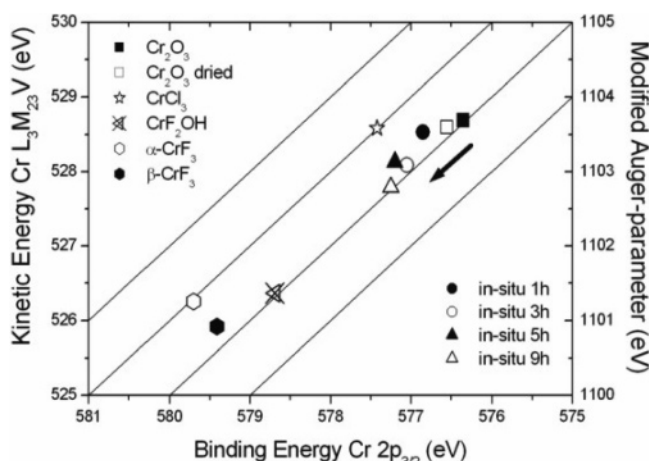


Figure 12. Chemical state plot for Cr $2p_{3/2}$ of Cr_2O_3 samples activated at $390\text{ }^\circ\text{C}$ ("in situ").

The results presented in the chemical state plot for Cl $2p_{3/2}$ (cf. Figure 11) can be interpreted in the similar way as for F 1s (cf. Figure 10). The inactive catalyst also possesses at the uppermost surface highly negative chloride ions with Cl $2p_{3/2}$ BE of 198.55 eV. These chloride ions are bound on the surface. The Cl $2p_{3/2}$ BE increases to 198.80 eV after chlorination proceeds further to the subsurface region. When the catalyst is activated by CCl_2F_2 at $390\text{ }^\circ\text{C}$ for 24 h, Cl $2p_{3/2}$ BE increases further to 199.05 eV. Since the modified Auger parameters of Cl $2p_{3/2}$ shift to lower values, the extra atomic relaxation energy changes and the increase in Cl $2p_{3/2}$ BE cannot be discussed simply in terms of initial state terms. However, Figure 14 shows that the Cl surface species are different than CrCl_3 .

Similar chemical state plots were obtained for the samples activated at $300\text{ }^\circ\text{C}$ providing similar information for the inactive and active catalysts (for details see ref 28). Similar results were also obtained by a so-called "in situ" analysis. The respective relative surface concentrations of F, Cr, O, and Cl are given in Table 3. By drying of the chromia and partial dehydroxylation, the BE of Cr $2p_{3/2}$ increases from 576.35 to 576.55 eV (cf. Figure 12). After 1 h dismutation of CCl_2F_2 , the catalyst was still inactive with a surface composition of 1.5 at. % fluoride and 2.4 at. % chloride and the Cr $2p_{3/2}$ BE shifts further by 0.30 eV. When the surface composition reached 4.5 at. % fluoride and 6.1 at. % chloride, the maximum activity was

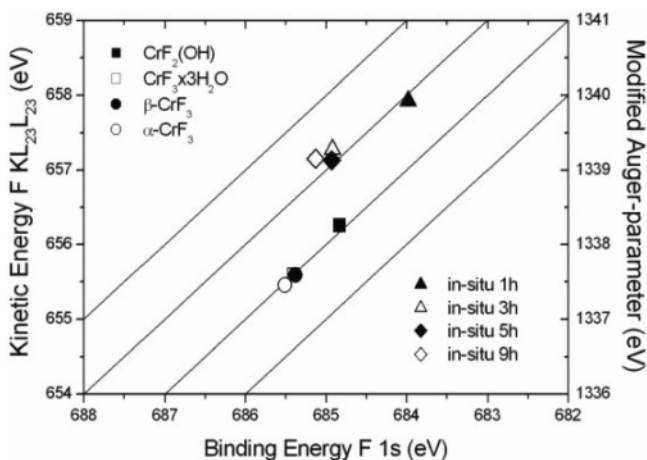


Figure 13. Chemical state plot for F 1s of Cr_2O_3 samples activated at 390°C (“in situ”).

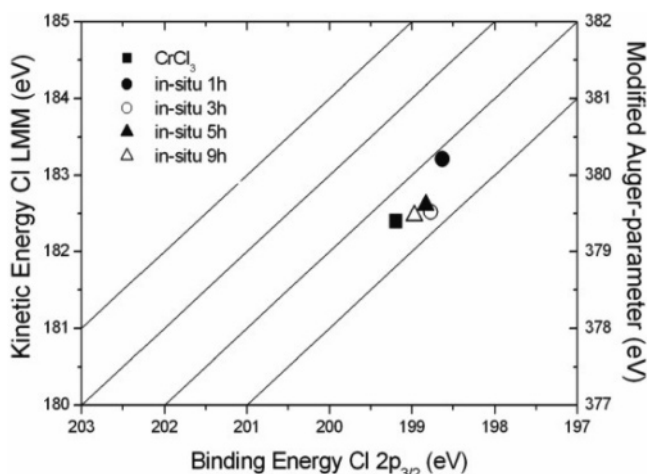


Figure 14. Chemical state plot for Cl $2p_{3/2}$ of Cr_2O_3 samples activated at 390°C (“in situ”).

TABLE 3: “In Situ” XPS Surface Composition (at. %) of Cr_2O_3 Catalysts Activated with CCl_2F_2 Dismutation Reaction at 390°C

time (h)	F	Cr	O	Cl	F + Cl	activity of catalyst
0	0	42.7	57.3	0	0	inactive
1	1.5	41.5	54.6	2.4	3.8	inactive
3	4.5	40.6	48.8	6.1	10.6	fully active
5	5.2	41.0	47.6	6.2	11.4	fully active
9	6.1	39.5	48.1	6.4	12.5	fully active

TABLE 4: XPS Surface Composition (at. %) of Cr_2O_3 Catalysts Treated with HF at 390°C

time (min)	F	Cr	O
15	11.5	41.5	47.0
60	11.6	41.4	47.0
180	11.8	42.5	45.8
540	13.7	40.9	45.4

achieved. Prolongation of the reaction up to 9 h raises the fluorine and chlorine surface concentrations content slightly to 6.1 and 6.4 at. %, respectively. The Cr $2p_{3/2}$ BE increases to 577.25 eV. For all of these samples the change in the modified Auger parameter α' may be considered as insignificant so that considering the samples in their initial states indicates that the electron density in the metal atom is reduced by the incorporation of halides.

The chemical state plots for F 1s and Cl $2p_{3/2}$ clearly show the difference between the inactive and active catalysts (cf. Figures 13 and 14). The inactive catalysts presented at the low

TABLE 5: XPS Surface Composition (at. %) of Cr_2O_3 Catalysts Treated with HCl at 390°C

time (min)	Cr	O	Cl
15	42.0	51.9	6.1
60	42.9	51.8	5.3
180	42.6	53.1	4.2
540	40.7	51.2	8.1

TABLE 6: XPS Surface Composition (at. %) of Cr_2O_3 Catalysts Prehalogenated before Halogen Treatment or Dismutation of CCl_2F_2 at 390°C

time (min)	F	Cr	O	Cl	F + Cl
15 min HF/15 min HCl	2.3	40.8	50.3	6.7	8.9
15 min HCl/15 min HF	8.9	41.1	48.9	1.1	10.0
15 min HF/60 min CCl_2F_2	5.7	40.1	48.8	5.4	11.1
15 min HCl/60 min CCl_2F_2	4.1	39.4	50.0	6.5	10.6

binding energy side on the plots possess highly negative halide ions that are strongly bound to the surface.

The catalyst becomes catalytically active when further fluoride and chloride ions are imbedded into the subsurface region. The increase in F 1s and Cl $2p_{3/2}$ BE indicates that the electron density is reduced at the halide ions. It is also clearly seen that the activated catalysts are very different from the reference samples. As a result, the same conclusion as was drawn from ex situ XPS analysis for the activated chromia was also obtained for the “in situ” study. The similarity of results obtained by ex situ and “in situ” XPS analysis for activated chromia suggest that a careful sample preparation by avoiding extended exposure to air provides reliable XPS results.

Fluorination and Chlorination of Chromia by HF and HCl, Respectively. To check the saturation limit of halogenation on chromia surface, the dried chromia was treated separately with HF and HCl, as well.

After drying and dehydroxylation, treatment with HF causes chromia to be fluorinated as normally expected. Within 15 min, 11.5 at. % fluorination takes place at the chromia surface. Further treatment with HF does not increase significantly the fluorine concentration. After 540 min of HF treatment, the fluorine content on the surface has reached 13.7 at. % (cf. Table 4).

It is clearly seen that the fluorination of the chromia surface takes place very fast at the beginning, the first 15 min of which is also the time to reach the maximum activity in the dismutation reactions of CCl_2F_2 at 390°C . Then the surface reaches a saturation point, and further surface fluorination with HF proceeds very slowly. Some of the surface oxygen can also be substituted with the fluoride ions after the OH groups are removed from the surface, but this seems to be a rather slow process when compared with the OH/F exchange reactions. It is interesting to note that the saturation concentration of ca. 11 at. % fluoride at the chromia is equal to the total halogen concentration at the catalyst surface in the dismutation reaction of CCl_2F_2 at the same temperature. This means that the fluoride ions occupy all the surface sites which in a CFC atmosphere are shared by both kind of halogen, F and Cl. In the XPS analysis a single F 1s peak is found for all of the HF treated samples around 685.0 eV BE (cf. Figure 16). This means that only one unique type of F species is observed in the samples. The XPS surface composition of the 15 min HF treated sample is $\text{CrO}_{1.13}\text{F}_{0.28}$. These results and the Cr $2p_{3/2}$ vs Cr LMM chemical state plot (cf. Figure 15) indicate that at the surface of chromia, after HF treatment at 390°C of chromium(III) oxide, fluorides are formed. HF treatment of chromia up to 540 min does not convert it into detectable, crystalline CrF_3 .

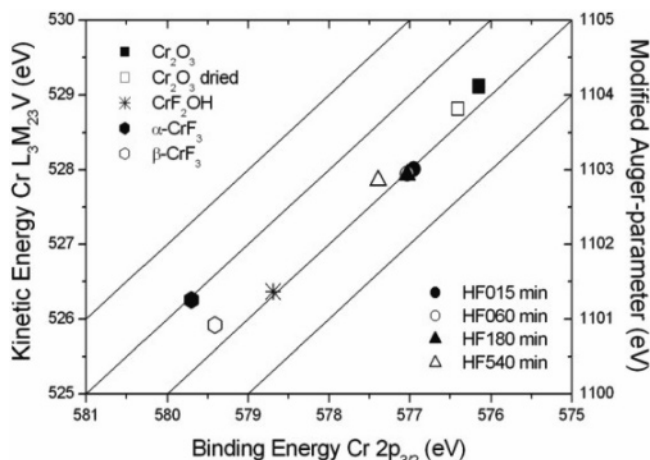


Figure 15. Chemical state plot for Cr $2p_{3/2}$ of Cr_2O_3 treated with HF at 390°C .

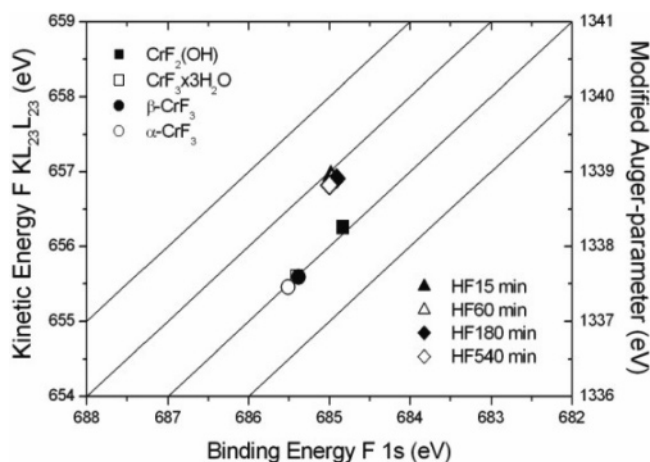


Figure 16. Chemical state plot for F $1s$ of Cr_2O_3 treated with HF at 390°C .

In the same way a treatment with HCl for 15 min results approximately in 6 at. % chlorination at the chromia surface. Further chlorination also proceeds slowly and after 540 min HCl treatment ca. 8 at. % was found at the surface (cf. Table 5). The fluctuations in the chlorine concentrations can be accounted for the errors which might result at least from the quantitative XPS analysis (10–20 at. %³⁰). The similar interpretation as it was done for the fluorination of chromia with HF, can be done for the chlorination of chromia with HCl. The surface OH and O are substituted by Cl ions, but this exchange process results lower halogenation at the surface when compared with the fluorination by HF. The chlorine concentration on the chromia surface by HCl treatment was found significantly less than the fluorine concentration of HF treated chromia. However, it was almost equal to the chlorine concentration which was obtained at the chromia surface by the CCl_2F_2 activation reactions after reaching the maximum activity. This means that with HCl treatment the Cl ions are not able to occupy all the surface sites which are accessible for F ions at the chromia surface. These differences might be due to both, thermodynamic and even more kinetic reasons (diffusion into the deeper surface region).

The XPS Cl $2p$ spectrum could be fitted as one doublet with an intensity ratio of 2:1. One type of Cl bond is observed in the samples and therefore, only a single species or phase is to be expected. For all of the Cl $2p_{3/2}$ BEs the value of ca. 198.8 eV is found (cf. Figure 18). Furthermore, the Cr $2p_{3/2}$ BEs are found between 576.9 and 577.3 eV (cf. Figure 17). These are

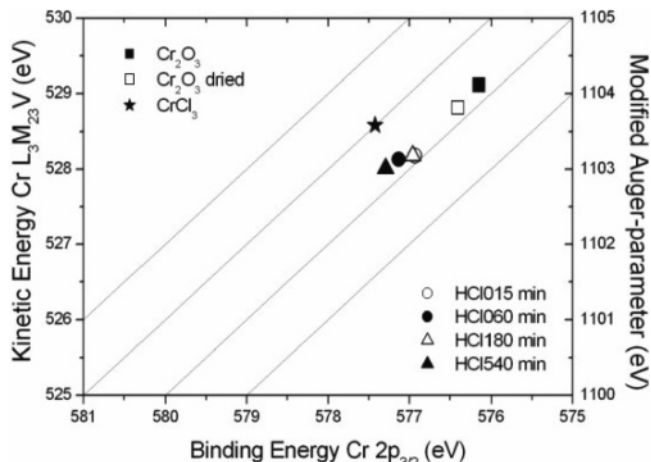


Figure 17. Chemical state plot for Cr $2p_{3/2}$ of Cr_2O_3 treated with HCl at 390°C .

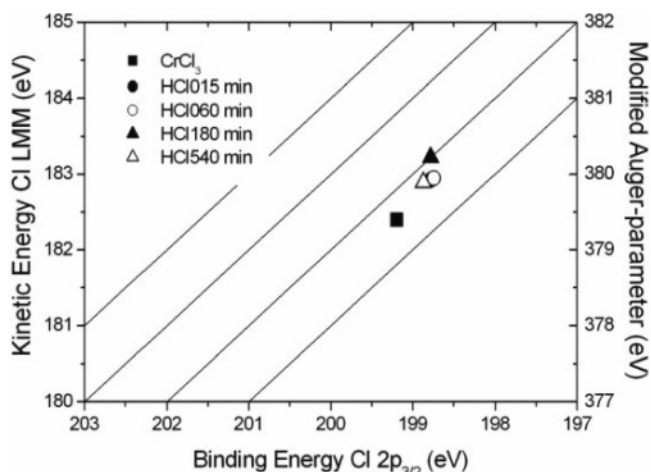


Figure 18. Chemical state plot for Cl $2p_{3/2}$ of Cr_2O_3 treated with HCl at 390°C .

higher than the BE of Cr $2p_{3/2}$ for Cr_2O_3 but they are very close to the BE of Cr $2p_{3/2}$ for CrCl_3 . The Auger parameters of Cr $2p_{3/2}$ for CrCl_3 and HCl treated samples show a gradual difference. This difference is an indication for that the treated samples are different from CrCl_3 . The XPS surface composition of the 15 min HCl treated sample is $\text{CrO}_{1.24}\text{Cl}_{0.14}$. Most probably oxide chlorides are formed with HCl treatment at 390°C on the chromia surface.

The Role of Surface Fluorine and Chlorine in Halogen Exchange Reactions. To find out whether the Cr–F and Cr–Cl bonds obtained by HF and HCl treatment, respectively, are exchangeable, prefluorinated or prechlorinated chromia samples were treated with HCl and HF, respectively, or reacted with CCl_2F_2 (cf. Table 6). It is important to check whether the prefluorination (or prechlorination) of the surface hinders the following chlorination (or fluorination).

Kemnitz et al.²⁰ showed in one study that in the presence of chlorofluorocarbons, HCl is formed and strongly adsorbed on the surface as HCl or active Cr–Cl type. Moreover, a second kind of chlorine, which is inactive chloride bonded to chromium, is formed.

Thomson et al.^{4,31} employed tracer techniques to differentiate the exchange activity of the halogen deposited on the γ -alumina as a result of conditioning. They found two kinds of chloride on the surface, (i) a mobile chloride which was very active toward exchange and which could be transferred into the gas

molecule and (ii) an inert chloride which was so strongly bound in the solid that it was incapable of undergoing any exchange reaction.

Rowley et al.³² showed clearly the formation of surface chlorine containing species during the catalytic fluorination of chlorofluoroethanes over fluorinated chromia. Independent from the origin of the chlorine, HCl or $\text{CF}_3\text{CCl}_2\text{F}$, the overall behavior of the chlorine containing species formed was identical indicating two types of surface species that are present. As the formation of catalytically inactive fluorine is the result of gradual replacement of $\text{Cr}^{\text{III}}-\text{O}$ by $\text{Cr}^{\text{III}}-\text{F}$,³³ an analogous process leads to catalytically inactive chlorine.

The [^{36}Cl] chlorine measurements on fluorinated chromia indicate that there is a turnover of chlorine between the catalyst and reacting chlorofluoroethane but no large increase in the chlorine content of the catalyst during its working life. Under a continuous flow of HF much of the active chlorine would be converted to chromium(III) fluoride.³⁴

After 15 min HCl treatment of prefluorinated chromia, the surface contains interestingly more chloride than fluoride. First for 15 min at 390 °C with HF treated chromia contains ca. 11 at. % fluoride. However, the following HCl treatment replaces the fluoride on the surface and reduces the fluorine content on the chromia surface to 2.3 at. %. Besides this, 6.7 at. % chlorine was found at the surface. On the other hand, a chromia sample prechlorinated for 15 min at 390 °C with HCl can just be chlorinated in the surface up to ca. 6 at. % Cl. Treatment of this sample for 15 min at 390° with HF results in higher fluoride content on the surface. Only 1.1 at. % chloride remained on the chromia surface, but 8.9 at. % fluoride was found. Obviously, both halogens can replace each other but to a different extent, depending on the course of reaction. That means that HCl can partly replace fluoride ions in prefluorinated chromia but HF can replace chloride ions to a greater but not full extent in prechlorinated chromia by substitution. In addition, separately with HF and HCl, respectively, pretreated chromia samples, following used for the dismutation reaction of CCl_2F_2 at 390° for 60 min yielded almost the same surface concentrations as it was obtained at the chromia surface when the maximum activity was reached with the dismutation reaction of CCl_2F_2 . The CCl_2F_2 molecule, which contains an equal number of fluorine and chlorine atoms, is at the same time a fluorination and chlorination agent for Cr_2O_3 in Cl/F exchange reactions. The last halogenation replaces the first one. In full agreement with the findings of Winfield et al.,^{32,35} there are mobile Cr–F and Cr–Cl bonds at the surface, and therefore the catalytic exchange reaction can take place by direct involvement of these bonds. The prefluorination does not obstruct the following chlorination on chromia surfaces and in the similar way prechlorination does not hinder the following fluorination of the surface, although fluorine can enter into surface sites which are not accessible for chlorine. In this manner the mobile Cr–F bond can be replaced by Cr–Cl bond and vice versa.

4. Conclusion

On the basis of different spectroscopic methods in combination with catalytic reactions, a comprehensive figure on processes occurring in the course of chromia activation for heterogeneously catalyzed halogen exchange may be drawn.

A. Change of Electron Density and Binding Energy as a Result of Chromia Halogenation. For Cr(III) 2p XPS, a fingerprint approach for chemical state identification should use the BE of the absolute maximum of Cr 2p_{3/2} as well as the BE and intensity of the 2p_{1/2} satellite around BE = 600 eV. To

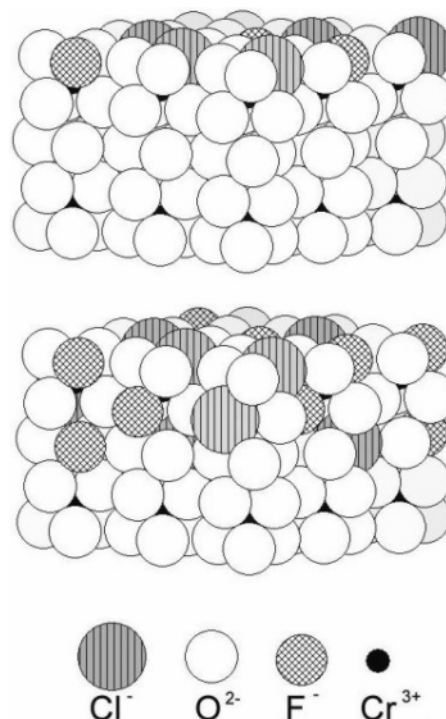


Figure 19. Model of inactive (top) and active (bottom) catalysts.

derive chemical state information, any Cr 2p spectrum of chromium(III) compounds must be definitely measured comprising the respective satellite features, i.e., using a sufficiently broad energy window up to ~ 610 eV.

An analysis of Cr 3s spectra also may provide an approach for fingerprinting chemical states of chromium(III) compounds, but the approach suffers from low Cr 3s intensity.

From the chemical point of view, the present study provides quantitative information about the inactive and active stages of the chromia catalyst which is used for the Cl/F exchange reactions and a model of the catalyst's surface chemistry (cf. Figure 19). The pyridine FTIR–photoacoustic analysis shows that the catalytic Cl/F exchange reaction takes place on the Lewis acid sites. The chromia catalyzed dismutation reaction of CCl_2F_2 , which is a Cl/F exchange reaction causes the catalyst surface to be fluorinated and chlorinated at the same time. The wet chemical analysis and the quantitative XPS results reveal that the halogenation takes place merely on the surface. The Cr K-edge XANES analysis performed in transmission mode also indicates that the halogenation takes place at the very surface near region. The crystalline bulk properties of chromia are not significantly changed with the activation or halogen treatment.

The low binding energies of the F 1s and Cl 2p core levels in the precatalytic sample and the symmetric peaks in the XP spectra indicate one major component. These represent the formation of a coordinatively unsaturated surface species, may be via exchange of OH groups with halogens during the early stages of halogenation. These species are bound to the exposed Lewis acid sites and to the other surface defects initially present on the chromia surface. They might be bridged or terminal.

B. The Catalytically Active Sites at the Halogenated Chromia Surface. The active sites and intrinsic defects on the chromia initiate the halogenation of the catalyst. As soon as the catalyst is halogenated, the dismutation reaction starts, but it is no longer competitive with the formation process at the beginning. When the OH groups are totally exchanged at the catalyst surface, the catalyst reaches to its maximum activity and the dismutation reaction dominates as the halogenation of

the chromia turns to be to a very slow process by integrating into the subsurface region. After this stage, fluorination proceeds slowly further (mainly diffusion-controlled) as the chlorination reaches to saturation.

According to the pyridine FTIR-photoacoustic analysis, increasing halogenation levels raise the Lewis acidity of the catalyst further as the catalytic reaction proceeds. The XPS Cr 2p BE also increases. Nucleation of a CrF₃ or CrCl₃ was not detected. The accumulation of the fluorine and chlorine by the surface reaction with the chlorofluorocarbon results in chromium oxide halide structure at the surface. This is also supported by the observation of CrO_xCl_yF_z⁻ and CrCl_xF_y⁻ secondary fragment ions for the activated samples in static TOF-SIMS experiments. The formation of separated CrX₃ (X = Cl, F) phases was not found very probable because the characteristic fragment ion patterns of these phases cannot be identified in the static TOF-SIMS spectra of activated chromia.³⁶

The chloride and fluoride ions are bound to the same chromium metal constructing the chromium oxide chloride fluoride species. The quantitative XPS analysis show that the maximum catalytic activity is reached when the surface of chromia is approximately 4 at. % fluorinated and 6 at. % chlorinated as a result of dismutation reaction of CCl₂F₂ at 390 °C. Almost similar XPS results are also obtained for the samples activated at 300 °C and for "in situ" XPS analysis. The activation of the catalyst takes longer time at 300 °C, because the formation of the catalyst proceeds slower at that temperature.

C. Mixed Chromium Oxohalogenides Are the Catalytic Active Phases. HF and HCl treatment of chromia at 390 °C for 9 h, forms chromium oxide fluoride and chromium oxide chloride species at the sample surface, respectively. No conversion to CrF₃ and CrCl₃ was found.

Prefluorination does not obstruct the following chlorination on chromia surface and in the same way prechlorination does not hinder the following fluorination of the chromia surface. However, the different degree of halogen exchange depending on the way of chlorination/fluorination and vice versa, clearly proves that Cl ions cannot occupy all the sites which are available for F ions. Only the mobile Cr-F bonds can be replaced by Cr-Cl bonds and vice versa. Reliable results can be obtained for activated chromia by ex situ XPS analysis when careful sample preparation methods are performed for avoiding air contamination. Excluding the necessity of CrCl₃ species for the catalytic activity since it is known as an inert substance, the formation of CrF₃ is not required for the achievement of catalytic activity. Instead of this, CrO_(x-y-z)Cl_yF_z species are sufficient to induce the onset of the catalytic activity.

Acknowledgment. We thank Dr. Riesemeier (Federal Institute of Material Research and Testing (BAM), Laboratory I.4) for giving the opportunity to perform the XANES analysis at the *BAMline* at BESSY II. We also thank Dr. S. L. M. Schroeder (Institute of Science and Technology, UMIST, Molecular Materials Centre, University of Manchester,) and Dr.

L. Wilde (Institute for Applied Chemistry Berlin-Adlershof) for their valuable discussions and assistance in XANES analysis. We kindly acknowledge the financial support of Deutsche Forschungsgemeinschaft (Grant KE 489/16).

References and Notes

- (1) Brunet, S.; Requieme, B.; Matouba, E.; Barrault, J.; Blancard, M. *J. Catal.* **1995**, *152*, 70.
- (2) Ballinger, T. H.; Yates, J. T. *J. Phys. Chem.* **1992**, *96*, 1417.
- (3) Ballinger, T. H.; Smith, R. S.; Colson, S. D.; Yates, J. T. *Langmuir* **1992**, *8*, 2473.
- (4) Thomson, J.; Webb, G.; Winfield, J. *J. Mol. Catal.* **1991**, *67*, 117.
- (5) Thomson, J.; Webb, G.; Winfield, J.; Bonniface, D.; Shortman, C.; Winterton, N. *Appl. Catal., A* **1993**, *97*, 67.
- (6) Hess, A.; Kemnitz, E. *J. Fluorine Chem.* **1995**, *74*, 27.
- (7) Kemnitz, E.; Hess, A. *J. Prakt. Chem.* **1992**, *334*, 591.
- (8) Hess, A.; Kemnitz, E. *J. Catal.* **1994**, *149*, 449.
- (9) Kemnitz, E.; Winfield, J. M. In *Advanced Inorganic Fluorides*; Nakajima, T.; Zemva, B.; Tressaud, A., Eds.; Elsevier: Lausanne, Switzerland, 2000; pp 367-401.
- (10) Boese, O.; Unger, W. E. S.; Kemnitz, E.; Schroeder, S. L. M. *Phys. Chem. Chem. Phys.* **2002**, *4*, 2824.
- (11) *Powder Diffraction File. PDF-2 Database, Sets 1-45*; ICDD A6; Dataware Technologies Inc.: 1995.
- (12) Ratnasamy, P.; Leonard, A. J. *J. Phys. Chem.* **1972**, *76*, 1838.
- (13) Kemnitz, E.; Hess, A.; Rother, G.; Troyanov, S. *J. Catal.* **1996**, *159*, 332.
- (14) Adamczyk, B.; Hess, A.; Kemnitz, E. *J. Mater. Chem.* **1996**, *6*, 1731.
- (15) Wagner, C. D. *NIST Standard Reference Database (NIST X-ray Photoelectron Spectroscopy Database). Number 20*, 1.0 ed.; Springer-Verlag, Gaithersburg, MD, 1989.
- (16) Seah, M. P. *Surf. Interface Anal.* **2001**, *31*, 721.
- (17) Seel, F. *Angew. Chem.* **1964**, *76*, 532.
- (18) Kemnitz, E.; Menz, D. H. *Prog. Solid State Chem.* **1998**, *26*, 97.
- (19) Cerrato, G.; Del Favero, N.; Filippi, F.; Morterra, C.; Magnacca, G.; Folonari, C. V. *J. Chem. Soc., Faraday Trans.* **1993**, *89*, 135.
- (20) Kemnitz, E.; Kohne, A.; Grohmann, I.; Lippitz, A.; Unger, W. E. S. *J. Catal.* **1996**, *159*, 270.
- (21) Grunes, L. A. *Phys. Rev. B* **1983**, *27*, 2111.
- (22) Boese, O.; Adamczyk, B.; Fiedler, K.; Kemnitz, E. *Catal. Lett.* **1998**, *54*, 211.
- (23) Adamczyk, B.; Boese, O.; Weiher, N.; Schroeder, S. L. M.; Kemnitz, E. *J. Fluorine Chem.* **2000**, *101*, 239.
- (24) Kemnitz, E.; Hass, D.; Grimm, B. *Z. Anorg. Allg. Chem.* **1990**, *589*, 228.
- (25) Unveren, E.; Kemnitz, E.; Hutton, S.; Lippitz, A.; Unger, W. E. S. *Surf. Interface Anal.* **2004**, *36*, 92.
- (26) Wagner, C. D.; Joshi, A. *J. Electron Spectrosc. Relat. Phenom.* **1988**, *47*, 283.
- (27) Ascarelli, P.; Moretti, G. *Surf. Interface Anal.* **1985**, *7*, 8.
- (28) Unveren, E. Thesis, Humboldt-Universität zu Berlin, 2004. <http://dochostrz.hu-berlin.de/dissertationen/unveren-ercan-2004-04-23/PDF/Unveren.pdf>.
- (29) Veal, B. W.; Paulikas, A. P. *Phys. Rev. Lett.* **1983**, *51*, 1995.
- (30) Sigbahn, H.; Karlson, L.; Melhorn, W., Eds. *Handbuch der Physik*; Springer-Verlag: Berlin, 1982; Vol. 31, p 215.
- (31) Thomson, J.; Webb, G.; Winfield, J. *J. Mol. Catal.* **1991**, *68*, 347.
- (32) Rowley, L.; Webb, G.; Winfield, J.; McCulloch, A. *Appl. Catal., A* **1989**, *52*, 69.
- (33) Kijowski, J.; Webb, G.; Winfield, J. M. *Appl. Catal.* **1986**, *27*, 181.
- (34) Wartenberg, H. v. *Z. Anorg. Allg. Chem.* **1942**, *249*, 110.
- (35) Rowley, L.; Thomson, J.; Webb, G.; Winfield, J. M. *Appl. Catal., A* **1991**, *79*, 89.
- (36) Unveren, E.; Kemnitz, E.; Oran, U.; Unger, W. E. S. *J. Phys. Chem. B* **2004**, *108*, 15454.